


Within-lesion heterogeneity of subcortical DWI lesion evolution, and stroke outcome: A voxel-based analysis

Marco Duering^{1,*}, Ruth Adam^{1,*}, Frank A Wollenweber¹, Anna Bayer-Karpinska¹, Ebru Baykara¹, Leidy Y Cubillos-Pinilla¹ , Benno Gesierich¹, Miguel Á Araque Caballero¹, Sophia Stoecklein², Michael Ewers¹, Ofer Pasternak³ and Martin Dichgans^{1,4,5}

Abstract

The fate of subcortical diffusion-weighted imaging (DWI) lesions in stroke patients is highly variable, ranging from complete tissue loss to no visible lesion on follow-up. Little is known about within-lesion heterogeneity and its relevance for stroke outcome. Patients with subcortical stroke and recruited through the prospective DEDEMAS study (NCT01334749) were examined at baseline ($n = 45$), six months ($n = 45$), and three years ($n = 28$) post-stroke. We performed high-resolution structural MRI including DWI. Tissue fate was determined voxel-wise using fully automated tissue segmentation. Within-lesion heterogeneity at baseline was assessed by free water diffusion imaging measures. The majority of DWI lesions (66%) showed cavitation on six months follow-up but the proportion of tissue turning into a cavity was small ($9 \pm 13.5\%$ of the DWI lesion). On average, $69 \pm 25\%$ of the initial lesion resolved without any visually apparent signal abnormality. The extent of cavitation at six months post-stroke was independently associated with clinical outcome, i.e. modified Rankin scale score at six months (OR = 4.71, $p = 0.005$). DWI lesion size and the free water-corrected tissue mean diffusivity at baseline independently predicted cavitation. In conclusion, the proportion of cavitating tissue is typically small, but relevant for clinical outcome. Within-lesion heterogeneity at baseline on advanced diffusion imaging is predictive of tissue fate.

Keywords

Clinical outcome, diffusion tensor imaging, free water, stroke, subcortical infarction

Received 19 February 2019; Revised 27 June 2019; Accepted 28 June 2019

Introduction

Subcortical infarcts identified on diffusion-weighted imaging (DWI) have variable fates. Previous studies have shown that DWI lesions can result in complete tissue loss (cavitation), T2 hyperintense lesions without apparent tissue loss, or resolve without a visible lesion on follow-up MRI.^{1–10} However, these studies mostly did not consider heterogeneity within individual lesions. Conceivably, the degree of cavitation and conversion into T2-visible lesion might influence clinical outcome. Only one previous study distinguished between fully and partially cavitated infarcts, acknowledging that different parts of a DWI lesion can have different fates.⁷ However, clinical outcome was not considered.

¹Institute for Stroke and Dementia Research (ISD), University Hospital, LMU Munich, Munich, Germany

²Department of Radiology, University Hospital, LMU Munich, Munich, Germany

³Departments of Psychiatry and Radiology, Brigham and Women's Hospital, Harvard Medical School, Boston, MA, USA

⁴Munich Cluster for Systems Neurology (SyNergy), Munich, Germany

⁵German Center for Neurodegenerative Diseases (DZNE), Munich, Germany

*These authors contributed equally to this work.

Corresponding author:

Marco Duering, Institute for Stroke and Dementia Research, University Hospital, LMU Munich Feodor-Lynen-Str. 17, Munich 81377, Germany.
Email: marco.duering@med.uni-muenchen.de

Little is known about the factors that determine tissue fate after subcortical infarcts. The severity of periventricular white matter hyperintensities (WMH)³ and the spatial relationship to WMH¹⁰ were found to predict cavity formation. Another study found that a lower apparent diffusion coefficient within a DWI lesion predicts subsequent cavitation,⁵ suggesting that within-lesion heterogeneity might already be present in the subacute phase of stroke and detectable by diffusion (tensor) imaging.

In the current study, we examined the evolution of DWI lesions in stroke patients over 36 months with the following aims: (i) to characterize within-lesion heterogeneity of tissue fate by quantifying the lesion parts that appear cavitated, T2 hyperintense or normal at follow-up; (ii) to explore relationships between tissue fate and stroke outcome; and (iii) to identify baseline predictors of tissue fate. We hypothesized that (i) DWI lesions show a variable extent of cavitation at follow-up, (ii) that the extent of cavitation is associated with stroke outcome, and (iii) that baseline features predict tissue fate, in particular diffusion imaging metrics within the DWI lesion.

To address these aims, we obtained multimodal, isotropic high-resolution MR images in a prospective cohort of stroke patients with subcortical infarcts and followed these patients up to three years. We applied a voxel-based, rater-independent analysis as well as advanced diffusion modelling.

Subjects and methods

Study cohort

Patients with acute or subacute ischemic stroke (within one week from symptom onset) were recruited from the local stroke unit through the prospective DEDEMAS (Determinants of Dementia After Stroke, NCT01334749) study.^{11,12} Stroke subtypes were classified according to the Trial of Org 10172 in Acute Stroke Treatment (TOAST) classification¹³ using all available clinical information at baseline. Ninety-seven patients had a supratentorial infarct and were thus considered for study inclusion. Eighteen patients were excluded because of missing follow-up MRI scans at six months ($n=12$) or protocol violations ($n=6$). The analysis was restricted to patients with subcortical DWI lesions and available data at baseline as well as at six months post-stroke ($n=45$, Supplemental Figure 1). Twenty-eight patients were also rescanned at three years post-stroke.

All procedures were performed in compliance with the Declaration of Helsinki of 1975 (and as revised in 1983) and protocols were approved by the ethics committee of the medical faculty at Ludwig-Maximilians-Universität Munich. Written informed consent was obtained from each patient.

MRI acquisition

All MRI scans (baseline and follow-ups at six months and three years' post-stroke) were obtained on a single 3T system (Magnetom Verio, Siemens Healthineers, Erlangen, Germany) with a 32-channel head coil. The standardized protocol included a 1 mm isotropic 3D T1-weighted sequence, a 1 mm isotropic 3D fluid-attenuated inversion recovery (FLAIR) sequence, 2 mm isotropic DWI (30 diffusion directions with a b-value of 1000 s/mm², 1 b = 0 image), a 2D T2-weighted sequence, and a gradient echo fieldmap (see online-only data supplement for detailed sequence parameters). Baseline examinations (including MRI) were performed within one week of symptom onset (median 4.2 days, interquartile range 2.7 days).

DWI lesion detection

Baseline DWI scans were corrected for susceptibility-induced distortions using the gradient echo fieldmap and the 'fugue' tool of the Functional Magnetic Resonance Imaging of the Brain Software Library (FSL, version 5.0.6).¹⁴ Head motion and eddy current-induced distortions were corrected using the FSL tool 'eddy_correct'.¹⁵ Next, the trace image (geometric mean of all DWI volumes) was calculated using MATLAB (version R2012b, The MathWorks, Inc). Infarct voxels were semi-automatically segmented on trace images by combining the FSL tissue segmentation tool 'fast'¹⁶ with an Otsu histogram segmentation¹⁷ implemented in MATLAB. If required, the resulting infarct map was manually edited to correct the segmentation (e.g. removal of artifacts) using a custom-written cluster-based software tool implemented in MATLAB.¹⁸

Assessment of tissue fate

The fate of tissue within DWI lesions was classified on follow-up scans into the following three classes: (1) cavitated, (2) hyperintense on T2, (3) normal appearing, i.e. no visible lesion. Cavitation was defined as a CSF-isointense signal^{19,20} on 3D-T1 images, since high resolution T1 images are known to have the highest sensitivity for cavitation.² Hyperintensity on T2 was determined on 3D-FLAIR images.

To analyze all imaging modalities in the same space, a half-way image was estimated from baseline and follow-up T1 scans using non-linear registration as implemented in the FSL tool 'fnirt'.²¹ Next, FLAIR and DWI were co-registered to half-way space.

For the voxel-based analysis, the segmentation into the three fate classes was performed automatically for every DWI lesion voxel using the FSL tissue segmentation tool 'fast' and Otsu histogram segmentation on images in half-way space. Individual DWI lesion

voxels were classified automatically on follow-up scans as cavitated, hyperintense or normal (Figure 1). All automated segmentations were visually checked, but no manual editing was conducted at this stage to avoid rater bias. We visually checked surrounding anatomical landmarks for signs of lesion/tissue shrinkage to ensure that results for tissue fates were not substantially biased by shrinkage. To obtain the extent (proportion) of each fate, the number of voxels classified as cavitated, hyperintense, or normal was divided by the total number of DWI lesion voxels.

We further classified individual DWI lesion voxels depending on whether there was a FLAIR hyperintense signal already on the baseline images.

For comparison, visual assessment of tissue fate was also conducted (see online-only data supplement).

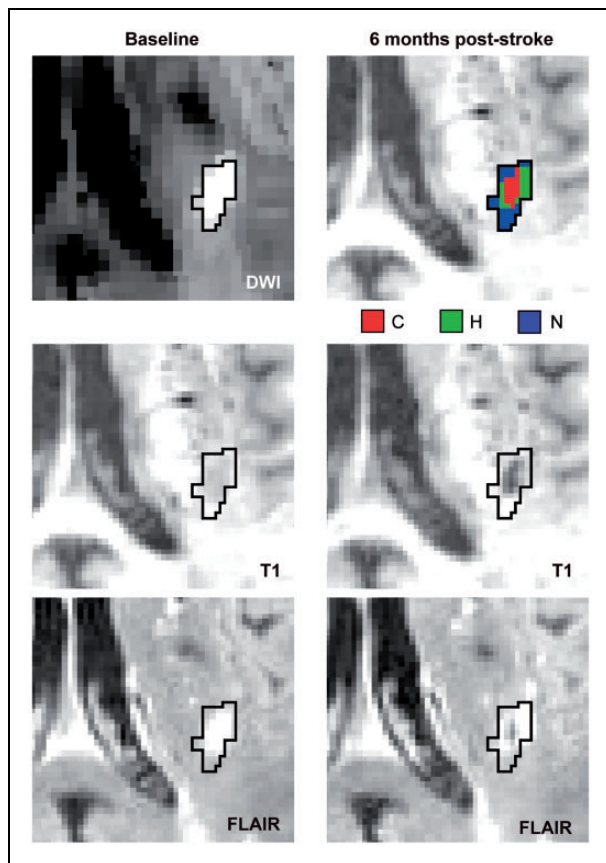


Figure 1. Heterogeneity of tissue fate within a DWI lesion followed over six months.

Baseline (left) and follow-up images (right) of an example DWI lesion. The margin was automatically identified on baseline DWI (trace image) and is marked by a black line. Voxels within this margin were classified into the following three classes using images obtained six months post-stroke. C: cavitation (red); H: T2 hyperintense (green); N: normal (blue).

White matter hyperintensity segmentation

White matter hyperintensities (WMH) as a marker for small vessel disease burden were segmented on baseline FLAIR images using the FSL tool ‘fast’ and subsequent Otsu segmentation. The segmentations were manually edited by a trained rater using a custom-written, cluster-based software tool implemented in MATLAB to remove artifacts.¹⁸ WMH volumes were normalized by intracranial volume as segmented on T2 images using the tissue segmentation algorithm²² in SPM12 (Statistical Parametric Mapping software toolkit, by the Wellcome Trust Centre for Neuroimaging). The inter-rater reliability for the resulting normalized WMH volume was excellent (intraclass correlation coefficient = 0.998).

Diffusion measures at baseline

Diffusion measures at baseline were estimated using the free water imaging toolbox running on MATLAB.^{23,24} In addition to providing conventional diffusion tensor measures such as mean diffusivity (MD), this method fits a two compartment model (free water compartment and tissue compartment) to estimate the free water fraction and the free water corrected tissue mean diffusivity (MDt). The free water compartment is modeled by an isotropic tensor with fixed diffusivity, reflecting freely diffusing extracellular water. The tissue compartment is the diffusion signal after eliminating free water. It reflects water restricted by tissue structures, such as intracellular water, and is modeled by a diffusion tensor fit. Conventional MD, free water corrected MDt and free water fraction were averaged across voxels that cavitated, across voxels that turned into a hyperintensity, and across voxels that turned into normal. Contralateral control regions were created by mirroring the DWI lesion in standard space (Montreal Neurological Institute, MNI-152).

Statistical analysis

All statistical tests were conducted using R (R software package, v.3.1.0; R Foundation for Statistical Computing, Vienna, Austria)²⁵ with each DWI lesion considered independently in the analyses.

The effects of tissue fate on clinical outcome six months post-stroke were determined by ordered logistic regressions (R package ‘ordinal’²⁶), with the modified Rankin scale score as dependent variable. Independent variables in simple regression models included the proportion of cavitation six months post-stroke and the following baseline variables: age, sex, NIHSS score, time between symptom onset and MRI scan, proportion of voxels appearing T2 hyperintense on baseline scans and DWI lesion size. Odds ratios were calculated

per standard deviation change. For multiple regressions, we used least absolute shrinkage and selection operator (lasso) variable selection (R package ‘glmnet’²⁷). This analysis was restricted to the subset of patients with a single subcortical DWI lesion ($n=25$) since the effects of multiple lesions with different fates are difficult to model.

Non-parametric regression (simple and multiple, R package ‘robustbase’, version 0.92-5²⁸) was used to identify predictors for tissue fate since the Shapiro–Wilk test and Q–Q plots of the residuals suggested non-normal distribution for most variables. The following baseline parameters were considered as independent variables: age, sex, smoking (past or current, when more than six months), hypertension, diabetes, time between stroke onset and MRI scan, proportion of voxels appearing T2 hyperintense on baseline scans, DWI lesion size, normalized WMH volume (as a marker of cerebral small vessel disease), the presence of high-grade stenosis ($\geq 70\%$, NASCET criteria) in extra- or intracranial arteries (as a marker of large artery disease), and the presence of atrial fibrillation (as a marker of cardiac pathology). The proportion of cavitated and hyperintense voxels served as dependent variables (separate analyses). For multiple regressions, we used lasso variable selection. All analyses were repeated for a subset of patients having a single subcortical DWI lesion ($n=25$).

The effects of baseline diffusion tensor measures on tissue fate were determined using simple ordered logistic regressions. Independent variables included average MD, MDt, and the free water fraction within regions that were cavitated, hyperintense and normal appearing on follow-up. The dependent variable was tissue fate ordered according to severity (cavitated > hyperintense > normal appearing). DWI lesion size and proportion of hyperintense voxels at baseline were added as covariates in multiple ordered logistic regressions. Again, all analyses were repeated for the subset of patients having a single subcortical DWI lesion ($n=25$).

Results

Baseline characteristics

The demographic and clinical characteristics of the 45 stroke patients are provided in Table 1. Overall, there were 59 subcortical DWI lesions (see Supplemental Figure 2 for lesion probability map). The most frequent underlying etiology was small vessel disease (31.1% of patients). In addition to MRI at six months post-stroke (all 45 patients), 28 patients (34 subcortical DWI lesions) had follow-up-imaging at three years post-stroke. There was no cavitation of DWI lesions on baseline scans. All DWI lesions showed some degree

of T2/FLAIR hyperintensity at baseline. The proportion of voxels appearing T2 hyperintense on baseline scans ($n=59$ lesions) was $44 \pm 26\%$ (mean \pm SD).

Tissue fate

Using automated segmentation of MR scans obtained six months post-stroke, 39 (66%) DWI lesions were classified as showing some degree (≥ 1 voxel) of cavitation, 15 (25%) DWI lesions were classified as being hyperintense on T2/FLAIR-weighted images without cavitation, and in 5 DWI lesions (9%) the initial lesion was no longer detectable (Figure 2(a)). Visual rating-based classification (see online-only data supplement) showed poor inter-rater agreement (Cohen’s kappa = 0.263).

Using automated segmentation and voxel-wise analysis, the proportion of cavitation within cavitated lesions ($n=39$) was low (group mean \pm SD: $13 \pm 15\%$ of the initial DWI lesion volume). Considering all DWI lesions ($n=59$), the proportion of voxels showing cavitation, hyperintensity, and appearing normal was $9 \pm 13.5\%$, $22 \pm 21\%$, and $69 \pm 25\%$, respectively (Figure 2(b)). Similar results were obtained when restricting the analysis to subjects with a single subcortical DWI lesion ($n=25$, cavitation: $8.5 \pm 12\%$; hyperintensity: $19.1 \pm 16\%$; normal: $72.4 \pm 23\%$). Focusing on the subgroup of patients with follow-up until three years post-stroke ($n=34$ lesions) revealed similar tissue fates at six months and three years post-stroke (Supplemental Figure 3).

Tissue fate is independently associated with clinical outcome

To explore the potential relevance of tissue fate for clinical outcome as assessed by the modified Rankin scale (mRS), we next performed ordered logistic regression analyses with mRS at six months post-stroke as the dependent variable and the proportion of cavitation as an independent variable. We further considered age, sex, baseline NIHSS, time between stroke onset and MRI scan, DWI lesion size, and the proportion of T2-hyperintense DWI lesion voxels at baseline as independent variables. To exclude interactions between multiple lesions with different fates, we focused on patients with a single subcortical DWI lesion ($n=25$).

In simple regressions analyses, the significant predictors for mRS at six months were DWI lesion size at baseline (OR = 6.66, 95% CI = 1.45–30.67, $p=0.01$), the proportion of T2-hyperintense DWI lesion voxels at baseline (OR = 2.71, 95% CI = 1.17–6.27, $p=0.02$), and the proportion of cavitation at six months post-stroke (OR = 4.71, 95% CI = 1.59–14.00, $p=0.005$) (Figure 3). In multiple regression analysis

Table 1. Characteristics of the study cohort.

	Six months follow-up (n = 45)	Three years follow-up (n = 28)
Demographic characteristics		
Age at baseline, mean (SD, range) [years]	73 (7.9, 53–82)	75 (7.4, 55–82)
Male, n (%)	32 (71)	19 (68)
Stroke etiology (TOAST classification), n (%)		
Large artery atherosclerosis, extracranial	5 (11.1)	2 (7.1)
Large artery atherosclerosis, intracranial	4 (9)	3 (10.7)
Cardioembolism	5 (11.1)	4 (14.3)
Small vessel occlusion	14 (31.1)	9 (32.1)
Stroke of other determined etiology	0 (0)	0 (0)
Competing etiologies (two or more causes)	6 (13.3)	4 (14.3)
Stroke of undetermined etiology	11 (24.4)	6 (21.4)
Vascular risk factors, n (%)		
Smoking (past or current, >6 months)	23 (51.1)	13 (46.4)
Hypertension	25 (55.6)	16 (57.1)
Hypercholesterolemia	21 (46.7)	11 (39.3)
Diabetes	9 (20)	5 (17.9)
Clinical scores, median (IQR)		
Modified Rankin Scale, before stroke	0 (0)	0 (0)
Modified Rankin Scale, baseline	2 (2)	1 (1.5)
Modified Rankin Scale, follow-up	1 (2)	0.5 (1)
NIHSS, baseline	3 (4)	2.5 (4)
Imaging characteristics		
Time from stroke onset to MRI, median (IQR) [days]	4.2 (2.7)	4.2 (2.8)
Subcortical DWI lesions per subject, median (range)	1 (1–3)	1 (1–2)
DWI lesion volume, median (IQR) [mm ³]	196 (811.5)	228.5 (773)
DWI lesion axial diameter, median (IQR) [mm]	9.6 (8.2)	9.8 (7.0)
Normalized WMH volume, median (IQR) [%]	0.41 (0.0068)	0.36 (0.0070)
Deep WMH score (Fazekas scale), median (IQR)	1 (1)	1 (1)

IQR: interquartile range; NIHSS: NIH Stroke Scale; TOAST: Trial of Org 10172 in Acute Stroke Treatment; WMH: white matter hyperintensities.

including all variables, lasso variable selection retained DWI lesion size and the proportion of cavitation in the model.

Predictors of infarct fate

Given the relevance of infarct fate for clinical outcome, we next explored potential baseline factors determining infarct fate. We performed linear regression analyses with age, sex, smoking, hypertension, diabetes, time between stroke onset and MRI scan, the proportion of T2-hyperintense voxels on baseline scans, and DWI lesion size as independent variables. We further included normalized WMH volume, the presence of high-grade stenosis in extra- or intracranial arteries, and the presence of atrial fibrillation as markers of vascular or cardiac pathology, respectively.

In simple regression analyses using the proportion of DWI lesion voxels with cavitation at six months post-stroke as the dependent variable, DWI lesion size (standardized $\beta=0.45$, $t=6.05$, $p=1.21 \times 10^{-7}$) and the proportion of T2-hyperintense DWI lesion voxels on baseline scans ($\beta=0.31$, $t=3.46$, $p=0.001$) were the only significant predictors (Figure 4). In multiple regression, lasso variable selection retained DWI lesion size in the final model (adjusted $R^2=0.36$). Similar results were obtained in patients with a single subcortical DWI lesion ($n=25$, see online-only data supplement). DWI lesion volume was also weakly associated with the proportion of normal appearing voxels at six months ($p=0.015$). We found no significant baseline predictors for the proportion of voxels appearing hyperintense at six months post-stroke.

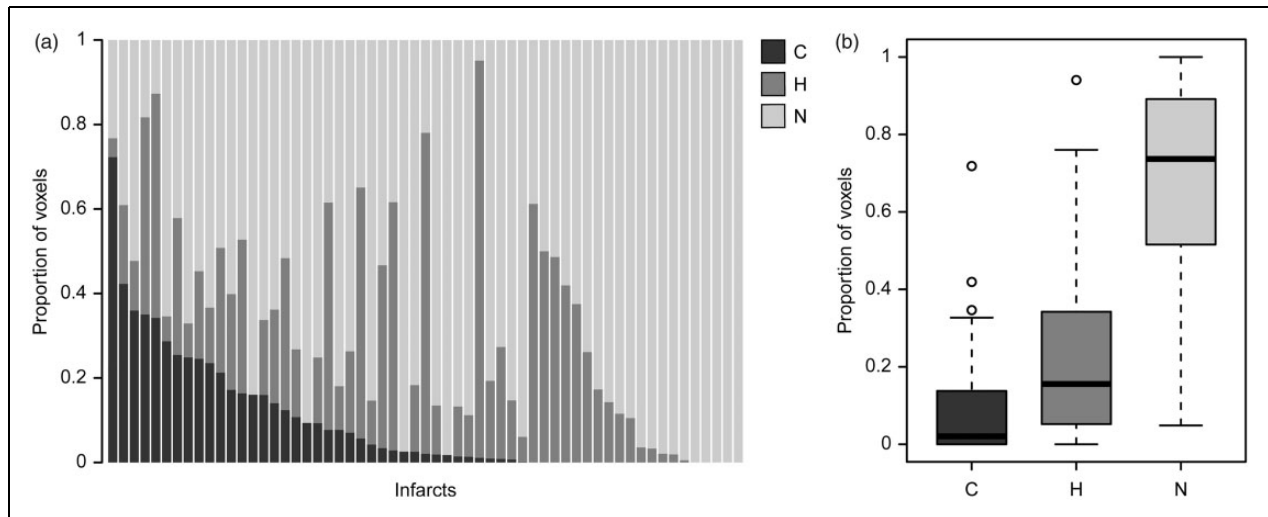


Figure 2. Tissue fate at six months post-stroke. Proportions of DWI lesion voxels appearing cavitated (C), hyperintense (H), and normal (N) six months post-stroke. (a) Results for individual DWI lesions ($n=59$). Lesions are arranged from left to right by decreasing extent of cavitation. (b) Boxplots for the whole sample of DWI lesions.

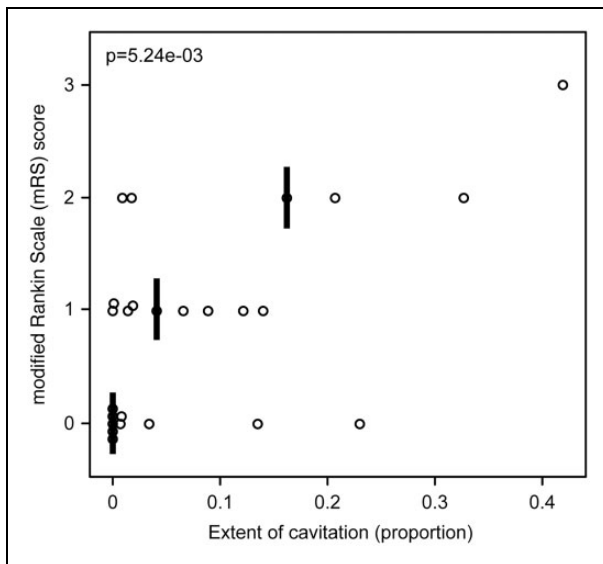


Figure 3. The extent of cavitation predicts clinical outcome. Swarm plots showing the distribution of modified Rankin scale scores at follow-up plotted against the proportion of DWI lesion voxels that turned into a cavitation at six months post-stroke. Vertical bars represent median values.

Within-lesion heterogeneity of diffusion measures at baseline predicts tissue fate

To determine whether the diffusion characteristics at baseline are predictive of tissue fate, we next explored whether DWI lesion regions that were cavitated, hyperintense, or normal appearing on follow-up differed in

their diffusion characteristics at baseline. We analyzed the conventional mean diffusivity (MD), the free water corrected MDt, and the free water fraction. Using ordinal logistic regression, conventional MD values showed no association with tissue fate ($p=0.90$). MDt values in DWI lesion regions were significantly associated with tissue fates in that lower MDt values were associated with more severe tissue fate (cavitation > hyperintensity > normal; OR = 0.69, 95% CI = 0.51–0.93, $p=0.016$) (Figure 5). There was a trend for an association between free water content and tissue fate (OR = 1.32, 95% CI = 0.96–1.82, $p=0.086$). Similar results were observed when controlling for DWI lesion size and the proportion of T2-hyperintense DWI lesion voxels on baseline scans (MD: OR = 1.02, 95% CI = 0.74–1.41, $p=0.90$; MDt: OR = 0.68, 95% CI = 0.49–0.95, $p=0.02$; Free water: OR = 1.34, 95% CI = 0.97–1.86, $p=0.07$). Similar results were further observed in patients with a single subcortical DWI lesion (see online-only data supplement).

Discussion

State-of-the-art neuroimaging enabled us to explore the fate of subcortical DWI lesions at an unprecedented level of detail. Our main findings can be summarized as follows: (1) While most subcortical DWI lesion showed some degree of cavitation over time, the proportion of tissue turning into a cavity was typically small, illustrating high within-lesion heterogeneity. On average, more than two-thirds of the initial DWI lesion resolved without any apparent signal abnormality on follow-up scans. (2) The proportion of cavitation

during follow-up was independently associated with clinical outcome six months post-stroke. (3) Within-lesion-heterogeneity was already detectable at baseline and was predictive of tissue fate; the free water corrected MDt was the most informative diffusion measure. Collectively, these findings contribute to our understanding of DWI lesion evolution and its association with clinical outcome.

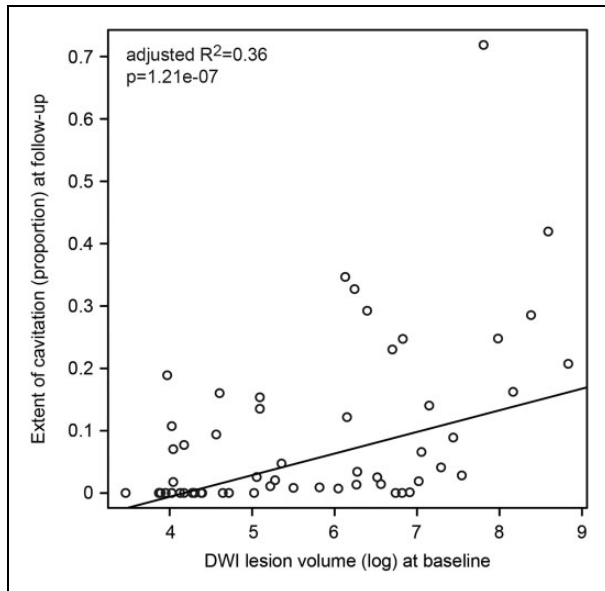


Figure 4. DWI lesion volume at baseline predicts the extent of cavitation at six months post-stroke.

Previous studies on infarct evolution provided highly variable results regarding the cavitation of subcortical DWI lesions over time, with figures ranging from 28% to 97% of lesions.^{1-5,7} Figures for DWI lesions that resolved without visible lesion on follow-up likewise varied from 5.3% to 30%.⁶⁻⁸ However, these studies assigned the entire lesion to a single category and thus did not account for within-lesion heterogeneity. We found that the part of an individual subcortical DWI lesion that cavitates or turns into a hyperintense lesion is often very small. Hence, technical aspects such as image resolution and variable criteria for classifying lesions into one or the other category may have influenced previous results. Of note, applying visual rating to our own data, the agreement between two experienced raters was relatively poor. Collectively, these findings highlight the advantage of voxel-based and rater-independent analyses.

We found tissue fate to be mostly determined within the first six months after stroke with little change from six months to three years post-stroke. This finding broadly agrees with a recent study that found no change for cavitation status between 3 and 15 months post-stroke, although that study did not consider within-lesion heterogeneity.⁵ Voxel-based studies with serial MRI over the first months after stroke are needed to characterize the temporal evolution of subcortical DWI lesions in more detail.

Our study highlights the importance of tissue fate for stroke outcome. Specifically, we found the proportion of cavitation to independently predict mRS scores at six months, thus adding to previous studies on outcome

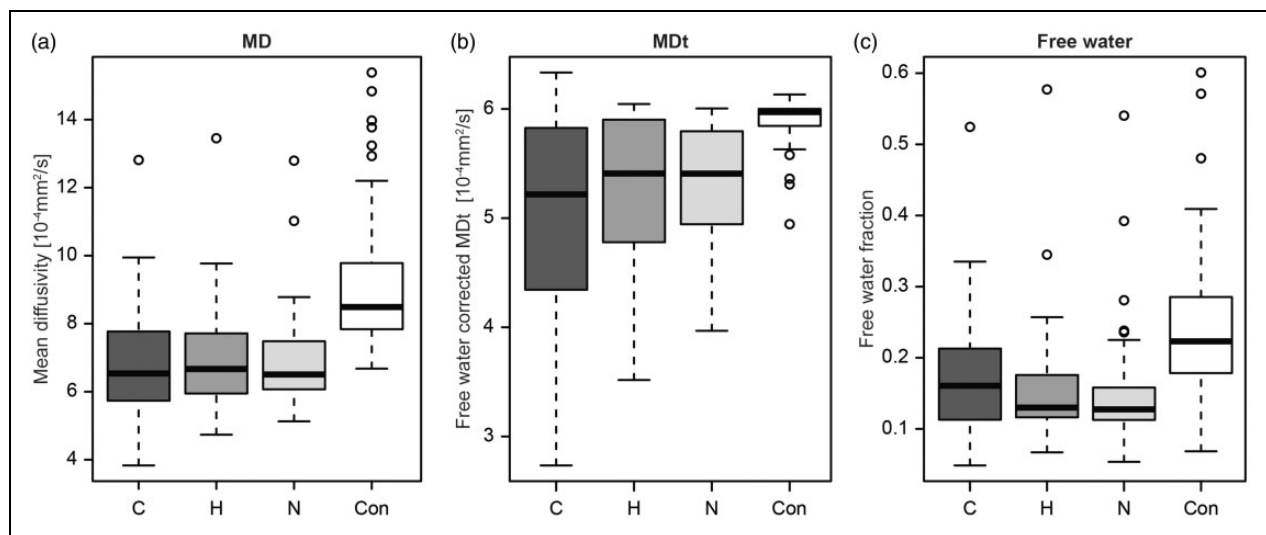


Figure 5. Diffusion measures at baseline predict tissue fate. Boxplots showing average values for mean diffusivity (MD, panel a), free water corrected tissue MD (MDt, panel b), and free water fraction (panel c) at baseline stratified according to tissue fates at six months post-stroke (C: cavitation; H: hyperintense; N: normal). Diffusion characteristics in contralateral control regions (Con) are shown for comparison.

predictors. Multiple regression analysis further retained DWI lesion size in the model. As such, our findings confirm and expand earlier findings on outcome predictors.^{29,30}

Given the clinical relevance of tissue cavitation, we searched for baseline predictors for cavitation on follow-up in our study. DWI lesion size and the free water corrected MDt at baseline were independent predictors. In contrast to a prior study,³ we found no influence of WMH volume on tissue fate. Also, we found no effect of the presence of large artery stenosis or of atrial fibrillation on cavitation at follow-up. This might indicate that the underlying vascular cause (e.g. cerebral small vessel disease or large artery stenosis of proximal blood vessels) does not have a major influence on tissue fate, although this would need to be examined in a targeted study with cerebral blood flow measurement in relevant arteries and vascular territories.

Our findings on within-lesion heterogeneity of DWI lesions at baseline and the observation that most voxels showing a diffusion restriction at baseline resolved without apparent MRI changes on follow-up add to the broader discussion whether subcortical DWI lesions represent irreversible tissue damage (infarct core). Some studies on larger infarcts including cortical infarcts suggest that the infarct core can be well represented by the DWI lesion,^{31,32} However, it has been demonstrated that DWI lesions can contain penumbra.³³ This is consistent with (partial) DWI lesion reversal after recanalization therapy in some patients as well as in animal models.^{34,35} In accord with our results, studies on subcortical infarcts consistently showed that the final infarct size on long term follow-up is typically smaller than the initial DWI lesion.^{3,7,8}

Advanced diffusion models, such as the free water imaging model allow characterizing the DWI lesion in more detail. While we found no difference in conventional MD between voxels with different fates, the free water corrected MDt was significantly lower in voxels that subsequently turned into a cavity. Lower MD in DWI lesions is commonly explained by cytotoxic edema,³⁶ i.e. a shift of water from the extracellular to intracellular space, where diffusion is more restricted. Our results on the free water corrected MDt suggest that more severe cytotoxic edema is indeed associated with a higher risk of cavitation, but this was only picked up after free water correction. The superiority of free water corrected diffusion measures over conventional measures in predicting tissue fate is likely based on the complexity of the diffusion signal and its temporal evolution in the acute and subacute phase of stroke. The free water imaging method allows separating cellular (tissue compartment) and extracellular (free water compartment) contributions to DWI.^{37,38} The free water

corrected MDt is expected to be more sensitive to cytotoxic edema affecting cellular restrictions.

Extracellular free water was overall reduced in DWI lesions compared with the contralateral hemisphere. Within lesions, however, we found a trend towards higher extracellular free water in voxels that subsequently cavitated. One explanation for this free water increase is vasogenic edema, which is accumulated in addition to cytotoxic edema in the subacute phase.^{39,40} Another explanation might be beginning tissue necrosis. Regardless of the exact source of the extracellular water increase, the conventional diffusion model cannot differentiate between cellular and extracellular water and the contribution of cytotoxic edema to the diffusion signal (decrease in diffusivity) is offset by the contribution of extracellular free water to the diffusion signal (increase in diffusivity). Hence, within-lesion heterogeneity in the subacute phase is not picked up by conventional diffusion imaging and is only unmasked after free water correction.

Limitations of our study include the variable time interval between symptom onset and baseline MRI. This might have resulted in some variability regarding diffusion characteristics, since both cytotoxic and vasogenic edemas are dynamic processes. Furthermore, the number of patients with follow-up data three years post-stroke and with a single subcortical DWI lesion was relatively low, resulting in limited power for some analyses. The inclusion of all stroke etiologies might limit comparability to the results of previous studies, which focused on cerebral small vessel disease. However, the broader scope of our study can also be regarded as a strength in terms of generalizability. Tissue shrinkage or focal atrophy occurring between baseline and follow-up might have biased the results on tissue fate, especially for the extent of cavitation. While we found no indication of shrinkage in surrounding structures, subtle atrophy might still have led to an underestimation of the extent of cavitation. As a main strength, we used a voxel-based approach for determination of tissue fate. This was enabled by the standardized imaging protocol with isotropic diffusion imaging and isotropic high-resolution 3D imaging for both T1 and FLAIR. Also, rater bias was excluded by automated tissue segmentation. Finally, application of the free water imaging allowed better characterization of the diffusion signal and predicting tissue fate.

Funding

The author(s) disclosed receipt of the following financial support for the research, authorship, and/or publication of this article: This study was supported by the Vascular Dementia Research Foundation, and by the national institutes of health (NIH, P41EB015902).

Declaration of conflicting interests

The author(s) declare no potential conflicts of interest with respect to the research, authorship, and/or publication of this article.


Authors' contributions

MDu: Study concept and design, data acquisition, data interpretation, drafting the manuscript, RA: study design, data analysis and interpretation, statistical analysis, drafting the manuscript, FAW: data acquisition, data interpretation, revisions of the manuscript, BG: data analysis and interpretation, revisions of the manuscript. BG, ABK, EB, LYC, MAA: data analysis, revisions of the manuscript. SS, ME, OP: data interpretation, revisions of the manuscript. MD: study supervision, data interpretation, drafting the manuscript.

Supplemental material

Supplemental material for this paper can be found at the journal website: <http://journals.sagepub.com/home/jcb>.

ORCID iD

Leidy Y Cubillos-Pinilla Wazna  <https://orcid.org/0000-0003-1535-8366>

References

- Benjamin P, Lawrence AJ, Lambert C, et al. Strategic lacunes and their relationship to cognitive impairment in cerebral small vessel disease. *Neuroimage Clin* 2014; 4: 828–837.
- Moreau F, Patel S, Lauzon ML, et al. Cavitation after acute symptomatic lacunar stroke depends on time, location, and MRI sequence. *Stroke* 2012; 43: 1837–1842.
- Koch S, McClendon MS and Bhatia R. Imaging evolution of acute lacunar infarction: leukoariorosis or lacune? *Neurology* 2011; 77: 1091–1095.
- Potter GM, Doubal FN, Jackson CA, et al. Counting cavitating lacunes underestimates the burden of lacunar infarction. *Stroke* 2010; 41: 267–272.
- Pinter D, Gattringer T, Enzinger C, et al. Longitudinal MRI dynamics of recent small subcortical infarcts and possible predictors. *J Cereb Blood Flow Metab*. Epub ahead of print 8 May 2018. DOI: 10.1177/0271678X18775215.
- Moreau F, Modi J, Almekhlafi M, et al. Early magnetic resonance imaging in transient ischemic attack and minor stroke: do it or lose it. *Stroke* 2013; 44: 671–674.
- Loos CMJ, Makin SDJ, Staals J, et al. Long-term morphological changes of symptomatic lacunar infarcts and surrounding white matter on structural magnetic resonance imaging. *Stroke* 2018; 49: 1183–1188.
- Kate MP, Riaz P, Gioia L, et al. Dynamic evolution of diffusion-weighted imaging lesions in patients with minor ischemic stroke. *Stroke* 2015; 46: 2318–2321.
- Loos CM, Staals J, Wardlaw JM, et al. Cavitation of deep lacunar infarcts in patients with first-ever lacunar stroke: a 2-year follow-up study with MR. *Stroke* 2012; 43: 2245–2247.
- Zhang X, Ding L, Yang L, et al. Relationship between white matter hyperintensities penumbra and cavity formation. *Med Sci Monit* 2016; 22: 41–49.
- Wollenweber FA, Zietemann V, Rominger A, et al. The determinants of dementia after stroke (DEDEMAS) study: protocol and pilot data. *Int J Stroke* 2014; 9: 387–392.
- Duering M, Righart R, Wollenweber FA, et al. Acute infarcts cause focal thinning in remote cortex via degeneration of connecting fiber tracts. *Neurology* 2015; 84: 1685–1692.
- Adams HP Jr, Bendixen BH, Kappelle LJ, et al. Classification of subtype of acute ischemic stroke. Definitions for use in a multicenter clinical trial. TOAST. Trial of Org 10172 in Acute Stroke Treatment. *Stroke* 1993; 24: 35–41.
- Jenkinson M, Beckmann CF, Behrens TE, et al. Fsl. *Neuroimage* 2012; 62: 782–790.
- Behrens TE, Woolrich MW, Jenkinson M, et al. Characterization and propagation of uncertainty in diffusion-weighted MR imaging. *Magn Reson Med* 2003; 50: 1077–1088.
- Zhang Y, Brady M and Smith S. Segmentation of brain mr images through a hidden markov random field model and the expectation-maximization algorithm. *IEEE Transac Med Imag* 2001; 20: 45–57.
- Otsu N. A thresholding selection method from gray-level histogram. *IEEE Transac Syst Man Cybernet* 1979; 9: 62–66.
- Baykara E, Gesierich B, Adam R, et al. A novel imaging marker for small vessel disease based on skeletonization of white matter tracts and diffusion histograms. *Ann Neurol* 2016; 80: 581–592.
- Gesierich B, Duchesnay E, Jouvent E, et al. Features and determinants of lacune shape: relationship with fiber tracts and perforating arteries. *Stroke* 2016; 47: 1258–1264.
- Wardlaw JM, Smith EE, Biessels GJ, et al. Neuroimaging standards for research into small vessel disease and its contribution to ageing and neurodegeneration. *Lancet Neurol* 2013; 12: 822–838.
- Andersson JLR, Jenkinson M and Smith S. Non-linear registration, aka spatial normalisation. *FMRIB Techn Rep* 2010. <https://www.fmrib.ox.ac.uk/datasets/techrep/tr07ja2/tr07ja2.pdf>.
- Ashburner J and Friston KJ. Unified segmentation. *Neuroimage* 2005; 26: 839–851.
- Pasternak O, Sochen N, Gur Y, et al. Free water elimination and mapping from diffusion MRI. *Magn Reson Med* 2009; 62: 717–730.
- Duering M, Finsterwalder S, Baykara E, et al. Free water determines diffusion alterations and clinical status in cerebral small vessel disease. *Alzheimers Dement* 2018; 14: 764–774.
- R Core Team. R: a language and environment for statistical computing. *R Foundation for Statistical Computing, Vienna, Austria*. www.R-project.org/ (2015, accessed 13 July 2019).

26. Christensen RHB. Ordinal: regression models for ordinal data, <https://CRAN.R-project.org/package=ordinal> (2015, accessed 19 August 2018).
27. Friedman JH, Hastie T and Tibshirani R. Regularization paths for generalized linear models via coordinate descent. *J Statist Software* 2010; 33: 1–22.
28. Maechler M, Rousseeuw P, Croux C, et al. Robustbase: basic robust statistics R package, <http://CRAN.R-project.org/package=robustbase> (2017, accessed 19 August 2018).
29. Helenius J, Mayasi Y and Henninger N. White matter hyperintensity lesion burden is associated with the infarct volume and 90-day outcome in small subcortical infarcts. *Acta Neurol Scand* 2017; 135: 585–592.
30. Asdaghi N, Pearce LA, Nakajima M, et al. Clinical correlates of infarct shape and volume in lacunar strokes: the secondary prevention of small subcortical strokes trial. *Stroke* 2014; 45: 2952–2958.
31. Campbell BC, Purushotham A, Christensen S, et al. The infarct core is well represented by the acute diffusion lesion: sustained reversal is infrequent. *J Cereb Blood Flow Metab* 2012; 32: 50–56.
32. Purushotham A, Campbell BC, Straka M, et al. Apparent diffusion coefficient threshold for delineation of ischemic core. *Int J Stroke* 2015; 10: 348–353.
33. Guadagno JV, Warburton EA, Aigbirhio FI, et al. Does the acute diffusion-weighted imaging lesion represent penumbra as well as core? A combined quantitative PET/MRI voxel-based study. *J Cereb Blood Flow Metab* 2004; 24: 1249–1254.
34. Yi KS, Choi CH, Lee SR, et al. Sustained diffusion reversal with in-bore reperfusion in monkey stroke models: confirmed by prospective magnetic resonance imaging. *J Cereb Blood Flow Metab* 2017; 37: 2002–2012.
35. Soize S, Tisserand M, Charron S, et al. How sustained is 24-hour diffusion-weighted imaging lesion reversal? Serial magnetic resonance imaging in a patient cohort thrombolized within 4.5 hours of stroke onset. *Stroke* 2015; 46: 704–710.
36. von Kummer R and Dzialowski I. Imaging of cerebral ischemic edema and neuronal death. *Neuroradiology* 2017; 59: 545–553.
37. Albi A, Pasternak O, Minati L, et al. Free water elimination improves test-retest reproducibility of diffusion tensor imaging indices in the brain: a longitudinal multi-site study of healthy elderly subjects. *Hum Brain Mapp* 2017; 38: 12–26.
38. Pasternak O, Westin CF, Bouix S, et al. Excessive extracellular volume reveals a neurodegenerative pattern in schizophrenia onset. *J Neurosci* 2012; 32: 17365–17372.
39. Loubinoux I, Volk A, Borredon J, et al. Spreading of vasogenic edema and cytotoxic edema assessed by quantitative diffusion and T2 magnetic resonance imaging. *Stroke* 1997; 28: 419–426.
40. Simard JM, Kent TA, Chen M, et al. Brain oedema in focal ischaemia: molecular pathophysiology and theoretical implications. *Lancet Neurol* 2007; 6: 258–268.